2021 60th IEEE Conference on Decision and Control (CDC)
December 13-15, 2021. Austin, Texas

Event-Driven Receding Horizon Control of Energy-Aware Dynamic Agents for Distributed Persistent Monitoring

Shirantha Welikala and Christos G. Cassandras

Abstract— **This paper addresses the persistent monitoring problem defined on a network where a set of nodes (targets) needs to be monitored by a team of dynamic energy-aware agents. The objective is to control the agents' motion to jointly optimize the overall agent energy consumption and a measure of overall node state uncertainty, evaluated over a finite period of interest. To achieve these objectives, we extend an established event-driven Receding Horizon Control (RHC) solution by adding an optimal controller to account for agent motion dynamics and associated energy consumption. The resulting RHC solution is computationally efficient, distributed and on-line. Finally, numerical results are provided highlighting improvements compared to an existing RHC solution that uses energy-agnostic first-order agents.**

I. Introduction

We consider the problem of controlling a group of mobile *agents* deployed to monitor a finite set of "points of interest" (henceforth called *targets*) in a mission space. In particular, each agent follows second-order unicycle dynamics and each target has an "uncertainty" metric associated with its state that increases when no agent is monitoring (i.e., sensing or collecting information from) the target and decreases when one or more agents are monitoring it by dwelling in its vicinity. The goal is to optimally control each agent's motion so as to collectively minimize the overall agent energy consumption and a measure of target uncertainties - evaluated over a fixed period of interest. This problem setup is widely known as the *persistent monitoring* problem and it encompasses applications such as environmental sensing [1], surveillance [2], traffic monitoring [3], data collection [4], event detection [5] and energy management [6]. In order to suit different application scenarios, this persistent monitoring problem has been studied in the literature under different objective functions [7], agent dynamic models [8], [9] and target state dynamic models [10], [11].

This paper considers the class of persistent monitoring problems that assumes the shapes of trajectory segments (available for the agents to travel between targets) as predefined [4], [10], [12]. The goal is to optimize agent target visiting schedules (i.e., the sequence of targets to visit and respective dwell-times to be spent at visited targets) and agent controls over corresponding trajectory segments. The work in [10] sees this as a Persistent Monitoring on a Network (PMN) problem where targets and trajectory segments are modeled as nodes and edges of a network, respectively. Such PMN problems are significantly more complicated than the NP-hard traveling salesman problems [13] and thus have motivated many different solution approaches [8], [10], [12].

The work in [12] proposes a centralized off-line greedy algorithm to determine the optimal target visiting schedules of agents in PMN problems. In contrast, for the same task, [10] proposes a gradient-based distributed on-line approach which, however, requires a brief centralized off-line initialization stage to address non-convexities. An alternative approach is taken in the recent work [8] which exploits the event-driven nature of PMN systems to develop a distributed on-line solution based on event-driven Receding Horizon Control (RHC) [14]. This RHC solution enjoys many promising features such as being computationally cheap, parameter-free, gradient-free and robust in the presence of various forms of state and system perturbations.

However, the work mentioned above [8], [10], [12] ignores agent dynamics by assuming each trajectory segment has a predefined transit-time value that an agent has to spend in order to travel on it. This assumption allows one to focus on determining the optimal target visiting schedules of agents, ignoring how the agents are governed during the transition periods where they travel on trajectory segments. In essence, it is identical to assuming each agent follows a first-order dynamic model controlled by its velocity.

In contrast, in this paper, we assume each agent follows a second-order dynamic model governed by acceleration rather than velocity. This leads to a better approximation of actual agent behaviors in practice and smoother agent state trajectories [9]. In particular, we incorporate agent energy consumption into the objective function to limit agent accelerations and velocities and also to motivate agents to make energy-efficient decisions. Under these modifications, we show how each agent needs to optimally select each transit-time value on its trajectory based on current local state information - instead of using a fixed set of predefined transit-time values. Moreover, we explicitly derive optimal control laws to govern each agent on each trajectory segment.

In this paper, first, we show that each agent's trajectory is fully characterized by the sequence of decisions it makes at specific discrete event-times in its trajectory. Second, considering an agent at each such event-time, we formulate a Receding Horizon Control Problem (RHCP) that determines the agent's optimal immediate control decisions over an *optimally determined* planning horizon. These control decisions are subsequently executed over a shorter action horizon defined by the next event that the agent observes, and the same process is continued in this event-driven manner. As

*Supported in part by NSF under grants ECCS-1931600, DMS-1664644, CNS-1645681, by AFOSR under grant FA9550-19-1-0158, by ARPA-E under grant DE-AR0001282 and by the NEXTCAR program under grant DE-AR0000796 and by the MathWorks.

The authors are with the Division of Systems Engineering and Center for Information and Systems Engineering, Boston University, Brookline, MA 02446, {shiran27,cgc}@bu.edu.

the third step, we show that this RHCP includes an optimal control component and the RHCP is then solved considering energy-aware second-order agents. Finally, several different numerical examples (PMN problems) are used to compare the developed RHC solution with respect to the RHC solution proposed in [8] that uses energy-agnostic first-order agents.

This paper is organized as follows. Section II presents the problem formulation and overview of the RHC approach. Section III presents the formulation and solution of the RHCP with second-order agents. Numerical results are provided in Section IV. Finally, Section V concludes the paper.

II. Problem Formulation

We consider a 2-dimensional mission space containing M targets (nodes) in the set $\mathscr{T} = \{1,2,\ldots,M\}$ where the location of target $i \in \mathscr{T}$ is fixed at $Y_i \in \mathbb{R}^2$. A team of N agents in the set $\mathscr{A} = \{1,2,\ldots,N\}$ is deployed to monitor the targets. Each agent $a \in \mathscr{A}$ moves within this mission space where its location and orientation at time t are denoted by $s_a(t) \in \mathbb{R}^2$ and $\theta_a(t) \in [0,2\pi]$, respectively.

a) ***Target Model****:* Each target $i \in \mathscr{T}$ has an associated *uncertainty state* $R_i(t) \in \mathbb{R}$ which follows the dynamics [10]:

$$\dot{R}_i(t) = \begin{cases} A_i - B_i N_i(t) & \text{if } R_i(t) > 0 \text{ or } A_i - B_i N_i(t) > 0 \\ 0 & \text{otherwise,} \end{cases} \quad (1)$$

where $N_i(t) = \sum_{a\in\mathscr{A}} \mathbf{1}\{s_a(t) = Y_i\}$ ($\mathbf{1}\{\cdot\}$ denotes the indicator function) is the number of agents present at target i at time t. According to (1): (i) $R_i(t)$ increases at a rate $A_i > 0$ when no agent is visiting target i, (ii) $R_i(t)$ decreases at a rate $A_i - B_i N_i(t)$ where $B_i > 0$ is the uncertainty removal rate by a visiting agent to the target i and (iii) $R_i(t) \geq 0, \forall t$.

b) ***Agent Model****:* The location $s_a(t)$ and orientation $\theta_a(t)$ of an agent $a \in \mathscr{A}$ follows the second-order unicycle dynamics given by

$$\dot{s}_a(t) = v_a(t)\begin{bmatrix}\cos(\theta_a(t))\\ \sin(\theta_a(t))\end{bmatrix},\ \dot{v}_a(t) = u_a(t),\ \dot{\theta}_a(t) = w_a(t), \quad (2)$$

where $v_a(t)$ is the tangential velocity, $u_a(t)$ is the tangential acceleration and $w_a(t)$ is the angular velocity. We consider $u_a(t)$ and $w_a(t)$ as the agent control inputs.

Note that according to (1), the agent has to stay stationary on a target $i \in \mathscr{T}$ for some positive amount of time to contribute to decreasing a positive target uncertainty $R_i(t)$. Therefore, during such a *dwell-time* period, the agent must enforce $u_a(t) = v_a(t) = 0$ with $s_a(t) = Y_i$.

c) ***Objective****:* Our aim is to minimize the composite objective J_T of the *total energy spent* J_e (called the *energy objective*) and the *mean system uncertainty* J_s (called the *sensing objective*) over a finite time interval $[0,T]$:

$$J_T = \underbrace{\alpha \int_0^T \sum_{a\in\mathscr{A}} u_a^2(t)\,dt}_{\triangleq J_e} + \underbrace{\frac{1}{T}\int_0^T \sum_{i\in\mathscr{T}} R_i(t)\,dt}_{\triangleq J_s}, \quad (3)$$

by controlling agent control inputs $u_a(t), w_a(t), \forall a \in \mathscr{A}, t \in [0,T]$. Note that α in (3) is a weight factor that can also be manipulated to constrain the resulting optimal agent controls (due to space limitations, details on selecting α to ensure proper normalization of the J_T components are provided in [15]). Note also that the cost of angular velocity (steering) control is not included in (3).

d) ***Graph Topology****:* We embed a directed graph topology $\mathscr{G} = (\mathscr{T}, \mathscr{E})$ into the mission space so that the *targets* are represented by the graph *vertices* $\mathscr{T} = \{1,2,\ldots,M\}$ and the inter-target *trajectory segments* are represented by the graph *edges* $\mathscr{E} \subseteq \{(i,j) : i,j \in \mathscr{T}\}$. These trajectory segments may take arbitrary (prespecified) shapes so as to account for constraints in the mission space and agent motion. We use ρ_{ij} to denote the *transit-time* that an agent spends on a trajectory segment $(i,j) \in \mathscr{E}$ to reach target j from target i. In contrast to [10] and [8] where these transit-time values were treated as predefined, in this work they are considered as control-dependent. We also use $\mathscr{P}_{ij}$ to represent the *transit-time interval* ($\mathscr{P}_{ij} \subset [0,T]$ of length ρ_{ij}) corresponding to the transit-time ρ_{ij}. The *neighbor set* and the *neighborhood* of a target $i \in \mathscr{T}$ are defined based on the available trajectory segments in $\mathscr{E}$ as $\mathscr{N}_i \triangleq \{j : (i,j) \in \mathscr{E}\}$ and $\bar{\mathscr{N}_i} = \mathscr{N}_i \cup \{i\}$.

e) ***Control****:* As stated earlier, when an agent $a \in \mathscr{A}$ dwells on a target $i \in \mathscr{T}$, the agent control $u_a(t)$ is zero. However, over such a dwell-time period, the agent control $w_a(t)$ may or may not be zero (exact details will be provided later). Next, when the agent is ready to leave the target i, it needs to decide the *next-visit* target $j \in \mathscr{N}_i$ along with the corresponding control profiles $u_a(t), w_a(t)$ to be used on the trajectory segment $(i,j) \in \mathscr{E}$ over $t \in \mathscr{P}_{ij}$.

In essence, the overall control exerted on an agent can be seen as a sequence of: *dwell-times* $\delta_i \in \mathbb{R}_{\geq 0}$, *next-visit* targets $j \in \mathscr{N}_i$ and *control profile segments* $\{(u_a(\tau), w_a(\tau)) : \tau \in \mathscr{P}_{ij}\}$. Our goal is to determine $(\delta_i(t_s), j(t_s), \{(u_a(\tau), w_a(\tau)) : \tau \in \mathscr{P}_{ij}(t_s)\})$ for any agent $a \in \mathscr{A}$ residing at any target $i \in \mathscr{T}$ at any time $t_s \in [0,T]$, which is optimal in the sense of minimizing (3).

f) ***Receding Horizon Control****:* As a solution to this PMN problem, inspired by the prior work [8] (where we dealt with first-order agents without agent energy concerns), this paper proposes an *Event-Driven Receding Horizon Controller* (RHC) at each agent. The key idea behind RHC derives from Model Predictive Control (MPC). However, RHC exploits the problem's event-driven nature to significantly reduce the complexity by effectively decreasing the frequency of control updates. As introduced and extended later on in [14] and [16], [8] respectively, the RHC is invoked by the agents in a *distributed* manner at specific events of interest in their trajectories. Upon invoking it, RHC determines the agent controls that optimize the objective (3) over a *planning horizon* and subsequently executes the determined optimal controls over a shorter *action horizon*.

In particular, when the RHC is invoked at some event-time $t_s \in [0,T]$ by an agent $a \in \mathscr{A}$ while residing at target $i \in \mathscr{T}$, it determines: (i) the remaining dwell-time $\delta_i(t_s)$ at target i, (ii) the next-visit target $j(t_s) \in \mathscr{N}_i$, (iii) the control profile segments $\{u_a(\tau), w_a(\tau) : \tau \in \mathscr{P}_{ij}(t_s)\}$ and (iv) the dwell-time $\delta_j(t_s)$ at target $j(t_s)$. These control decisions are jointly represented by $U_{ia}(t_s)$ and its optimal value is determined by solving an optimization problem of the form:

$$U_{ia}^*(t_s) = \underset{U_{ia}(t_s)\,\in\,\mathbb{U}(t_s)}{\arg\min}\ J_H(X_{ia}(t_s),U_{ia}(t_s);H)+\hat{J}_H(X_{ia}(t_s+H)),$$

where $X_{ia}(t_s)$ is the current local state and $\mathbb{U}(t_s)$ is the feasible control set at time t_s (exact definitions are provided later). The term $J_H(X_{ia}(t_s),U_{ia}(t_s);H)$ represents the immediate cost over the planning horizon $[t_s,t_s+H]$ and $\hat{J}_H(X_{ia}(t_s+H))$ is an estimate of the future cost based on the state at t_s+H. We follow the *variable horizon* concept proposed in [8] where the planning horizon length is treated as an upper-bounded function of control decisions $\mathsf{w}(U_{ia}(t_s)) \leq H$ rather than an exogenously selected value H, and the $\hat{J}_H(X_{ia}(t_s+H))$ term is ignored. Thus, this approach incorporates the selection of planning horizon length $\mathsf{w}(U_{ia}(t_s))$ into the above optimization problem, which now can be re-stated as

$$\begin{aligned} U_{ia}^*(t_s) = &\underset{U_{ia}(t_s)\,\in\,\mathbb{U}(t_s)}{\arg\min} \quad J_H(X_{ia}(t_s),U_{ia}(t_s);\ \mathsf{w}(U_{ia}(t_s)))\\ &\text{subject to} \quad \mathsf{w}(U_{ia}(t_s)) \leq H. \end{aligned} \tag{4}$$

1) Preliminary Results: According to (1), the target state (uncertainty) $R_i(t)$ of a target $i \in \mathscr{T}$ is piece-wise linear and its gradient $\dot{R}_i(t)$ changes only when one of the following (strictly local) *events* occurs: (i) an agent arrival at i, (ii) $R_i(t)$ switches from positive to zero, denoted as $[R_i(t) \to 0^+]$, or (iii) an agent departure from i. Let us denote the sequence of such event-times (associated with target i) as t_i^k where $k \in \mathbb{Z}_{>0}$ with $t_i^0 = 0$. Then, it is easy to see from (1) that

$$\dot{R}_i(t) = \dot{R}_i(t_i^k),\ \forall t \in [t_i^k, t_i^{k+1}). \tag{5}$$

Remark 1: As pointed out in [8], [17] (and the references therein), allowing multiple agents to simultaneously reside on a target (known also as "simultaneous target sharing") is known to lead to solutions with poor performance levels. Thus, we enforce a constraint on the controller to ensure [8]:

$$N_i(t) \in \{0,1\},\ \forall t \in [0,T],\ \forall i \in \mathscr{T}. \tag{6}$$

Clearly, this constraint only applies if $N \geq 2$.

Under (6), it follows from (1) and (5) that the sequence $\{\dot{R}_i(t_i^k)\}_{k=0,1,\ldots}$ is a *cyclic order* of three elements: $\{-(B_i - A_i), 0, A_i\}$. Next, in order to make sure that each agent is capable of enforcing the event $[R_i \to 0^+]$ at any target $i \in \mathscr{T}$, we assume the following simple stability condition [8]:

Assumption 1: Target uncertainty rate parameters A_i and B_i of each target $i \in \mathscr{T}$ satisfy $0 < A_i < B_i$.

a) ***Decomposition of the Sensing Objective*** J_s*:* The following theorem provides a target-wise and temporal decomposition of the sensing objective J_s defined in (3).

Theorem 1: ([8, Th.1]) The contribution to the term J_s in (3) by a target $i \in \mathscr{T}$ during a time period $[t_0,t_1) \subseteq [t_i^k, t_i^{k+1})$ for some $k \in \mathbb{Z}_{\geq 0}$ is $\frac{1}{T}J_i(t_0,t_1)$, where,

$$J_i(t_0,t_1) = \int_{t_0}^{t_1} R_i(t)dt = \frac{(t_1-t_0)}{2}[2R_i(t_0)+\dot{R}_i(t_0)(t_1-t_0)]. \tag{7}$$

b) ***Local Sensing Objective Function****:* The *local sensing objective function* of a target $i \in \mathscr{T}$ over a period $[t_0,t_1) \subseteq [0,T]$ is defined as

$$\bar{J}_i(t_0,t_1) = \sum_{j \in \bar{\mathscr{N}}_i} J_j(t_0,t_1), \tag{8}$$

where each $J_j(t_0,t_1)$ term is evaluated using Theorem 1.

c) ***Decomposition of the Energy Objective*** J_e*:* A similar decomposition result as Theorem 1 applies to the energy objective J_e defined in (3). The contribution to J_e by an agent $a \in \mathscr{A}$ from traversing a trajectory segment $(i,j) \in \mathscr{E}$ over the transit-time interval $[t_o,t_f] \triangleq \mathscr{P}_{ij}$ is $J_a(t_o,t_f)$, where,

$$J_a(t_o,t_f) = \int_{t_o}^{t_f} u_a^2(t)\,dt. \tag{9}$$

Note that the agent does not contribute to the J_e term during dwell-time intervals as $u_a(t) = 0$ during such periods.

d) ***Agent Angular Velocity Profile*** $w_a(t)$*:* The control profile segment $\{w_a(t) : t \in \mathscr{P}_{ij}\}$ that needs to be used by an agent $a \in \mathscr{A}$ over the transit-time interval $\mathscr{P}_{ij}$ on the trajectory segment $(i,j) \in \mathscr{E}$ can be obtained using only the following information: (i) the agent tangential acceleration profile $\{u_a(t) : t \in \mathscr{P}_{ij}\}$ and (ii) the shape of the trajectory segment (i,j) given in a parametric form $\{(x(p),y(p)) : p \in [p_o,p_f]\}$. Note that the parameter values p_o and p_f correspond to the terminal target locations Y_i and Y_j, respectively. For convenience, let us use the notation: $x'_p = \frac{dx(p)}{dp}$.

First, we require a minor technical assumption regarding the said trajectory segment shape parameterization.

Assumption 2: There exists an injective function $f : [p_o,p_f] \to [0,y_{ij}]$ such that $f(p) \triangleq \int_{p_o}^{p}\left((x'_p)^2+(y'_p)^2\right)^{\frac{1}{2}}dp$, with $f(p_f) = y_{ij}$ and a corresponding inverse function f^{-1}.

Second, let $F(p) \triangleq (x'_p y''_p - y'_p x''_p)/\left((x'_p)^2+(y'_p)^2\right)^{\frac{3}{2}}$ and $l_a(t)$ be the total distance the agent has traveled on the trajectory segment (i,j) by time t. Finally, notice that $l_a(t) = \int_{t_o}^{t} v_a(t)dt$ and $v_a(t) = \int_{t_o}^{t} u_a(t)dt,\quad \forall t \in [t_o,t_f] \triangleq \mathscr{P}_{ij}$ with terminal conditions: $l_a(t_f) = y_{ij}$ and $v_a(t_f) = 0$.

The following Theorem 2 allows us to dispense of $w_a(t)$ as an agent control by obtaining it in terms of $v_a(t)$. Note that, due to space limitations, all proofs are provided in [15].

Theorem 2: The required agent angular velocity profile $\{w_a(t) : t \in \mathscr{P}_{ij}\}$ on trajectory segment $(i,j) \in \mathscr{E}$ is

$$w_a(t) = F(f^{-1}(l_a(t)))\,v_a(t), \tag{10}$$

where $f(\cdot)$ and $F(\cdot)$ are the functions defined earlier.

Two example usages of this theorem are provided in [15].

e) ***The Equivalent Dynamic Agent Model****:* Since we now have discussed how an agent $a \in \mathscr{A}$ can control its angular velocity $w_a(t)$ (i.e., via (10)), we can omit angular dynamics from (2) to construct an equivalent dynamic agent model, that focuses only on the tangential dynamics on a trajectory segment $(i,j) \in \mathscr{E}$. In particular, upon taking the state vector as $[l_a(t),\ v_a(t)]^T$ for some $t \in \mathscr{P}_{ij}$, we can express the corresponding state dynamics as a second-order single-input linear system:

$$\begin{bmatrix}\dot{l}_a(t)\\ \dot{v}_a(t)\end{bmatrix} = \begin{bmatrix}0 & 1\\ 0 & 0\end{bmatrix}\begin{bmatrix}l_a(t)\\ v_a(t)\end{bmatrix} + \begin{bmatrix}0\\ 1\end{bmatrix}u_a(t). \tag{11}$$

2) *ED-RHC Problem (RHCP) Formulation:* Consider an agent $a \in \mathscr{A}$ residing on a target $i \in \mathscr{T}$ at some time $t_s \in [0,T]$. Recall that control $U_{ia}(t_s)$ in (4) includes *dwell-time* decisions δ_i and δ_j at the current target i and the next-visit target $j \in \mathscr{N}_i$, respectively. As shown in Fig. 1, a dwell-time decision δ_i (or δ_j) can be divided into two interdependent decisions: (i) the *active time* τ_i (or τ_j) and (ii) the *inactive* (or *idle*) *time* $\bar{\tau}_i$ (or $\bar{\tau}_j$). Therefore, the agent has to optimally choose *decision variables* which form the control vector $U_{ia}(t_s) = [\tau_i, \bar{\tau}_i, j, \{u_a(t)\}, \tau_j, \bar{\tau}_j]$. Note that here we have: (i) omitted representing each of these decision variable's dependence on t_s, (ii) used the notation $\{u_a(t)\}$ to represent $\{u_a(t) : t \in \mathscr{P}_{ij}(t_s)\}$ and (iii) omitted $\{w_a(t) : t \in \mathscr{P}_{ij}(t_s)\}$ as it can be found directly from $\{u_a(t)\}$ via (10).

a) ***The Receding Horizon Control Problem (RHCP)****:* Let us denote the real-valued component of the control vector $U_{ia}(t_s)$ in (4) as $U_{iaj}(t_s) = [\tau_i, \bar{\tau}_i, \{u_a(t)\}, \tau_j, \bar{\tau}_j]$. The discrete component of $U_{ia}(t_s)$ is simply the next-visit target $j \in \mathscr{N}_i$. In this setting (see also Fig. 1), we define the planning horizon length $\mathsf{w}(U_{ia}(t_s))$ in (4) as

$$\mathsf{w}(U_{iaj}(t_s)) \triangleq \tau_i + \bar{\tau}_i + \rho_{ij} + \tau_j + \bar{\tau}_j. \tag{12}$$

The current local state $X_{ia}(t_s)$ in (4) is considered as $X_{ia}(t_s) = [s_a, v_a, \theta_a, \{R_j : j \in \bar{\mathscr{N}}_i\}]$ (again, omitting the dependence on t_s). Then, the optimal controls are obtained by solving (4), which can be re-stated as the following set of optimization problems, henceforth called the RHC Problem (RHCP):

$$\begin{aligned} U^*_{iaj} = \quad & \underset{U_{iaj} \,\in\, \mathbb{U}}{\arg\min} \quad J_H(X_{ia}(t_s), U_{iaj};\ \mathsf{w}(U_{iaj}));\ \forall j \in \mathscr{N}_i, \\ & \text{subject to} \quad \mathsf{w}(U_{iaj}) \leq H, \end{aligned} \tag{13}$$

$$j^* = \underset{j \,\in\, \mathscr{N}_i}{\arg\min} \quad J_H(X_{ia}(t_s), U^*_{iaj};\ \mathsf{w}(U^*_{iaj})). \tag{14}$$

Note that (13) requires solving $|\mathscr{N}_i|$ optimization problems, one for each neighboring target $j \in \mathscr{N}_i$ ($|\cdot|$ is the cardinality operator). The next step (14) is a simple comparison to determine the optimal next-visit target j^*. Therefore, the final optimal controls of the RHCP are $U^*_{ia}(t_s) = [U^*_{iaj^*}, j^*]$.

The objective function $J_H(\cdot)$ in (13) is chosen to reflect the contribution to the main objective J_T in (3) by the targets in the neighborhood $\bar{\mathscr{N}}_i$ and by the agent a, over the planning horizon $[t_s, t_s + \mathsf{w}]$ as

$$J_H(X_{ia}(t_s), U_{iaj};\ \mathsf{w}) \triangleq \alpha_H \underbrace{J_a(t_o, t_f)}_{\triangleq J_{eH}} + \underbrace{\frac{1}{\mathsf{w}} \bar{J}_i(t_s, t_s + \mathsf{w})}_{\triangleq J_{sH}}. \tag{15}$$

where $\mathsf{w} = \mathsf{w}(U_{iaj})$ and $\alpha_H \triangleq \alpha$ (i.e., the weight factor used in (3)). In (15), the form of the J_{sH} component has been selected so that it is analogous to the J_s component in (3) (with T replaced by w). As illustrated in Fig. 1, note also that $t_e \triangleq t_s + \mathsf{w}$, $[t_o, t_f] \triangleq \mathscr{P}_{ij} \subseteq [t_s, t_e]$ and $\rho_{ij} \triangleq t_f - t_o$.

b) ***Planning Horizon****:* In conventional RHC methods, the RHCP objective function is evaluated over a fixed planning horizon length H, where H is selected exogenously. This makes the RHCP solution dependent on the choice of H. In contrast, through (15) and (12) above, we have

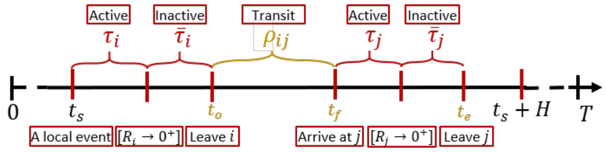

Fig. 1: Event timeline and control decisions in ED-RHC.

made the RHCP solution (i.e., (13) and (14)) free of the parameter H, by using H only as an upper-bound to the actual planning horizon length $\mathsf{w}(U_{iaj})$ in (12) and selecting H to be sufficiently large (e.g., $H = T - t_s$).

In fact, since the planning horizon length $\mathsf{w}(U_{iaj})$ is a control-dependent, the above RHCP formulation simultaneously determines the *optimal planning horizon* length $\mathsf{w}^* = \mathsf{w}(U^*_{iaj^*})$. Moreover, as shown in Fig. 1, the time to depart from the current target i (i.e., t_o), the time to arrive at the destination target j (i.e., t_f) and the corresponding transit-time $\rho_{ij} = t_f - t_o$, are also control-dependent. Hence, this RHCP formulation also determines the optimal values of each of these quantities: t^*_o, t^*_f and $\rho^*_{ij^*}$, respectively.

c) ***Overview of the RHCP Solution Process****:* Looking back at (7) and (8), notice that the sensing component J_{sH} of the RHCP objective (15) does not explicitly depend on the agent control profile segment $\{u_a(t) : t \in \mathscr{P}_{ij}\}$, but, it depends on the agent's transit-time ρ_{ij} value and on the other control decisions in U_{iaj}: $\tau_i, \bar{\tau}_i, \tau_j, \bar{\tau}_j$. Therefore, let us denote J_{sH} as a function parameterized by ρ_{ij}: $J_{sH}(\tau_i, \bar{\tau}_i, \tau_j, \bar{\tau}_j; \rho_{ij})$.

In contrast, based on (9), notice that the energy component J_{eH} of the RHCP objective (15) only depends on agent control profile segments, specifically on $\{u_a(t) : t \in \mathscr{P}_{ij}\}$. Therefore, let us denote J_{eH} simply as $J_{eH}(\{u_a(t)\})$.

As illustrated in Fig. 2, we exploit this property of the RHCP objective components (J_{sH} and J_{eH}) to solve the RHCP (13). In particular, we start with analytically solving the optimization problem which we label as RHCP(ρ_{ij}):

$$J^*_{sH}(\rho_{ij}) \triangleq \min_{(\tau_i, \bar{\tau}_i, \tau_j, \bar{\tau}_j) \,\in\, \mathbb{U}_s(\rho_{ij})} J_{sH}(\tau_i, \bar{\tau}_i, \tau_j, \bar{\tau}_j; \rho_{ij}). \tag{16}$$

For this purpose, we exploit a few results established in [8] where RHCP(ρ_{ij}) (16) has already been solved while treating ρ_{ij} as a known constant.

Next, we use the $J^*_{sH}(\rho_{ij})$ function obtained from (16) and the relationship $\rho_{ij} = t_f - t_o$ to reformulate the problem of optimizing the RHCP objective (15) as an optimal control problem (OCP):

$$[t^*_o, t^*_f, \{u^*_a(t)\}] = \underset{t_o,\, t_f,\, \{u_a(t)\}}{\arg\min} \quad \alpha_H J_e(\{u_a(t)\}) + J^*_{sH}(t_f - t_o). \tag{17}$$

Finally, as shown in Fig. 2, it is straightforward how the RHCP (13) solution U^*_{iaj} can be constructed from the obtained solutions of the OCP (17) and the RHCP(ρ_{ij}) (16).

d) ***Event-Driven Action Horizon****:* Each RHCP solution (i.e., $U^*_{ia}(t_s) = [U^*_{iaj^*}, j^*]$ from (13)-(14)) obtained over a planning horizon $\mathsf{w}(U^*_{iaj^*}) \leq H$ is generally executed over a shorter *action horizon* $h \leq \mathsf{w}(U^*_{iaj^*})$. In particular, the action horizon h is determined by the first event that takes place after t_s, the time when the RHCP was last solved. Such

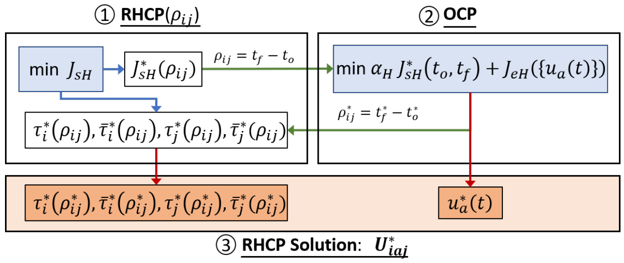

Fig. 2: Overview of the three-step RHCP solution process when solving (13) for some next-visit target $j \in \mathcal{N}_i$: 1. Solving the receding horizon control component of (13) (i.e., (16)); 2. Solving the optimal control component of (13) (i.e., (17)); 3. Constructing the final solution of (13).

a subsequent event may be *controllable* if it results from executing the last solved RHCP solution or *uncontrollable* if it results from a random or an external event (if allowed).

When executing the RHCP solution obtained by an agent at target i at time t_s, there are three mutually exclusive controllable events that may occur subsequently. They are:

1. Event $[h \to \tau^*_i]$*:* This event is feasible only if $\tau^*_i(t_s) > 0$ and it occurs at a time $t = t_s + \tau^*_i(t_s)$. If $R_i(t) > 0$, it coincides with a departure event from target i. Otherwise, i.e., if $R_i(t) = 0$, it coincides with a $[R_i \to 0^+]$ event.

2. Event $[h \to \bar{\tau}^*_i]$*:* This event is feasible if $\tau^*_i(t_s) = 0$ (when $R_i(t_s) = 0$) and $\bar{\tau}^*_i(t_s) \geq 0$. It occurs at $t = t_s + \bar{\tau}^*_i(t_s)$ and coincides with a departure event from target i.

3. Event $[h \to \rho_{ij^*}]$*:* This event is feasible only if a departure event (from target i) occurred at t_s. Clearly this event coincides with an arrival event at target $j^*(t_s)$.

In an agent trajectory, at a given time instant, only one of these three controllable events is feasible. However, there are two uncontrollable events that may occur at an agent residing in a target i due to two specific controllable events at a neighboring target $j \in \mathcal{N}_i$. These two types of events are aimed to enforce the "no simultaneous target sharing" condition (i.e., the control constraint (6)) and thus, they only apply to multi-agent problems. To enforce this condition, an agent at target i modifies its neighborhood $\mathcal{N}_i$ to $\mathcal{N}_i \backslash \{j\}$ when: (i) another agent already resides at target j or (ii) another agent is en-route to visit target j. Therefore, we define the following two *neighbor-induced events* at target i due to a neighbor $j \in \mathcal{N}_i$:

4. Covering Event C_j, $j \in \mathcal{N}_i$*:* This event causes $\mathcal{N}_i$ to be modified to $\mathcal{N}_i \backslash \{j\}$.

5. Uncovering Event $\bar{C}_j$, $j \in \mathcal{N}_i$*:* This event causes $\mathcal{N}_i$ to be modified to $\mathcal{N}_i \cup \{j\}$.

If one of these two events occurs while the agent is awaiting an event $[h \to \tau^*_i]$ or $[h \to \bar{\tau}^*_i]$, the RHCP is resolved to account for the updated neighborhood $\mathcal{N}_i$.

e) ***Three Forms of RHCPs****:* The exact form of the RHCP ((13)-(14)) that needs to be solved at a certain event-time depends on the event that triggered the end of the previous action horizon. In particular, corresponding to the three controllable event types, there are three RHCP forms:

RHCP1: At a target i and time t_s, this problem form is solved upon: (i) the arrival event or (ii) a C_j (or $\bar{C}_j$), $j \in \mathcal{N}_i$ event, when $R_i(t_s) > 0$.

RHCP2: At a target i and time t_s, this problem form is solved upon: (i) an event $[h \to \tau^*_i]$ or (ii) a C_j (or $\bar{C}_j$), $j \in \mathcal{N}_i$ event, when $R_i(t_s) = 0$. Thus, it is the same as **RHCP1** but with $\tau_i = 0$ (hence simpler).

RHCP3: At a target i and time t_s, this problem form is solved upon: (i) an event $[h \to \tau^*_i]$ with $R_i(t_s) > 0$ or (ii) an event $[h \to \bar{\tau}^*_i]$. Simply, this problem form is solved whenever the agent is ready to depart from the target. Therefore, it is the same as **RHCP1** but with $\tau_i = \bar{\tau}_i = 0$.

III. Solving Event-Driven RHCPs

1) Solution of ***RHCP3****:* **RHCP3** is the simplest RHCP given that $\tau_i = \bar{\tau}_i = 0$ in U_{ia} by default. Therefore, U_{iaj} (i.e., the real-valued component of U_{ia}, used in (13)) is limited to $U_{iaj} = [\{u_a(t)\}, \tau_j, \bar{\tau}_j]$ and the planning horizon $\mathsf{w}(U_{iaj})$ defined in (12) becomes $\mathsf{w}(U_{iaj}) = \rho_{ij} + \tau_j + \bar{\tau}_j$. Under these conditions, we next solve (13) (via solving RHCP(ρ_{ij}) (16) and OCP (17)) and (14) to obtain the **RHCP3** solution.

a) ***Solution of RHCP(***ρ_{ij}***)*** *(16):* As mentioned before, RHCP(ρ_{ij}) has already been solved in [8] - while treating ρ_{ij} as a known fixed value. In particular, the RHCP(ρ_{ij}) solution corresponding to the **RHCP3** takes the form [8, Th. 2]:

$$(\tau^*_j, \bar{\tau}^*_j) = \begin{cases} (0,0) & \text{if } D_1 > D_2 \text{ or } \bar{A} \geq B_j \\ (D_2, 0) & \text{else if } D_2 < D_3 \\ (D_3, 0) & \text{else if } B_j > \bar{A} \geq B_j \left[1 - \frac{\rho_{ij}^2}{(\rho_{ij}+D_3)^2}\right] \\ (D_3, \bar{D}_1) & \text{else if } \bar{D}_1 \leq \bar{D}_2 \\ (D_3, \bar{D}_2) & \text{otherwise,} \end{cases}$$
$$(\tau^*_i, \bar{\tau}^*_i) = (0,0) \quad \text{and} \quad J^*_{sH}(\rho_{ij}) = J_{sH}(\tau^*_j, \bar{\tau}^*_j; \rho_{ij}), \tag{18}$$

where $\bar{A} = \sum_{m \in \bar{\mathcal{N}}_i} A_m$, $D_1 = \frac{\bar{A}\rho_{ij}}{B_i - \bar{A}}$, $D_2 = \min\{D_3, \ H - \rho_{ij}\}$, $D_3 = \frac{R_j(t_o)}{B_j - A_j} + \frac{A_j}{B_j - A_j}\rho_{ij}$, $\bar{D}_1 = \sqrt{\frac{(B_j - A_j)(\rho_{ij}+D_3)^2 - B_j\rho_{ij}^2}{\bar{A}_j}} - (\rho_{ij} + D_3)$, $\bar{A}_j = \bar{A} - A_j$, $\bar{D}_2 = H - (\rho_{ij} + D_3)$, $\bar{R} = \sum_{m \in \bar{\mathcal{N}}_i} R_m$,

$$J_{sH}(\tau_j, \bar{\tau}_j; \rho_{ij}) = \frac{C_1\tau_j^2 + C_2\bar{\tau}_j^2 + C_3\tau_j\bar{\tau}_j + C_4\tau_j + C_5\bar{\tau}_j + C_6}{\rho_{ij} + \tau_j + \bar{\tau}_j},$$

$C_1 = \frac{1}{2}[\bar{A} - B_j]$, $C_2 = \frac{\bar{A}_j}{2}$, $C_3 = \bar{A}_j$, $C_4 = [\bar{R}(t_o) + \bar{A}\rho_{ij}]$, $C_5 = [\bar{R}_j(t_o) + \bar{A}_j\rho_{ij}]$, $\bar{R}_j \triangleq \bar{R} - R_j$, $C_6 = \frac{\rho_{ij}}{2}[2\bar{R}(t_o) + \bar{A}\rho_{ij}]$.

Note that in (18), not only J^*_{sH}, but also τ^*_j and $\bar{\tau}^*_j$ are functions of the transit-time ρ_{ij}. To provide intuition about the $J^*_{sH}(\rho_{ij})$ function form, let us consider the first case in (18) where $(\tau^*_j, \bar{\tau}^*_j) = (0,0)$ that results in $J^*_{sH}(\rho_{ij}) = J_{sH}(0,0;\rho_{ij}) = \bar{R}(t_o) + \frac{1}{2}\bar{A}\rho_{ij}$, under the condition $\bar{A} \geq B_j$ or $D_1 > D_2$. Using the coefficients stated below (18), it can be shown that $D_1 > D_2 \iff \rho_{ij} > \min\{\frac{R_j(t_o)(B_i - \bar{A})}{\bar{A}B_j - A_jB_i}, \ H(1 - \frac{\bar{A}}{B_i})\}$. From this example, it is clear that the function $J^*_{sH}(\rho_{ij})$ is dependent on the neighborhood parameters (e.g., $\bar{A}, B_j, B_i$) as well as the current neighborhood state (e.g., $\bar{R}(t_o)$, $R_j(t_o)$).

*b) **Objective Function of OCP** (17):* Note that we now have solved RHCP(ρ_{ij}) and have obtained the functions (of ρ_{ij}): $\tau_i^*, \bar{\tau}_i^*, \tau_j^*, \bar{\tau}_j^*$, and, most importantly, J_{sH}^*. Based on the RHCP solution process outlined in Fig. 2, our next step is to formulate and solve the corresponding OCP (17).

As seen in (17), the sensing objective component of OCP is $J_{sH}^*(t_f - t_o)$. Note that we now can explicitly express this term using the obtained $J_{sH}^*(\rho_{ij})$ function in (18) and the relationship $\rho_{ij} = t_f - t_o$. For notational convenience, taking into account that in **RHCP3** t_o is the current event-time when the RHCP is solved (i.e., $t_o = t_s$ where t_s is known), let us denote the sensing objective component of OCP as $\phi(t_f) \triangleq J_{sH}^*(t_f - t_o)$. On the other hand, using (15) and (9), the energy objective component of OCP (17) can be expressed as $J_{eH}(\{u_a(t)\}) = \int_{t_o}^{t_f} u_a^2(t)dt$.

*c) **Solution of OCP** (17):* In the following analysis, for notational convenience, we use $\dot{x} = Ax(t) + Bu(t)$ with $A = \begin{bmatrix} 0 & 1 \\ 0 & 0 \end{bmatrix}$, $B = \begin{bmatrix} 0 \\ 1 \end{bmatrix}$, $x(t) = \begin{bmatrix} l_a(t) \\ v_a(t) \end{bmatrix}$, $u(t) = u_a(t)$, to represent the agent dynamics stated in (11). Under this notation, the OCP (17) can be stated as

$$\begin{aligned} \min_{t_f, \{u(t)\}} \quad & \alpha_H \int_{t_o}^{t_f} u^2(t)dt + \phi(t_f) \\ \text{subject to} \quad & \dot{x} = Ax(t) + Bu(t), \\ & x(t_o) = [0,0]^T, \quad x(t_f) = [y_{ij}, 0]^T. \end{aligned} \tag{19}$$

The last two constraints in (19) are simply terminal constraints for the agent motion on the trajectory segment (i, j). Note that (19) is a standard free final time, fixed initial and final state optimal control problem. Hence, there is an established solution procedure [18] (see [15] for details).

Theorem 3: The optimal terminal time t_f^* of the OCP (19) satisfies the equation:

$$(t_f - t_o)^4 \frac{d\phi(t_f)}{dt_f} = 36\alpha_H y_{ij}^2, \tag{20}$$

where $\phi(t_f)$ is known and the corresponding optimal control law $u^*(t)$ is given by

$$u^*(t) = \frac{12y_{ij}}{(t_f^* - t_o)^3} \left[\frac{t_f^* + t_o}{2} - t \right], \ \forall t \equiv [t_o, t_f]. \tag{21}$$

Using the optimal terminal time t_f^* and control $u^*(t)$ (i.e., $u_a^*(t)$) given in Theorem 3, the optimal energy objective component of this OCP can be obtained as $J_{eH}(\{u_a^*(t)\}) = 12y_{ij}^2/(t_f^* - t_o)^3$. The corresponding optimal sensing objective component is $\phi(t_f^*) = J_{sH}^*(t_f^* - t_o)$ and the optimal transit-time value is $\rho_{ij}^* = t_f^* - t_o$.

*d) **Solution of RHCP** (13) **for** U_{iaj}^*:* As outlined in Fig. 2, we next conclude solving RHCP (13). First, we apply the determined ρ_{ij}^* value in (18) to get the optimal control decisions: τ_j^* and $\bar{\tau}_j^*$ of the control vector U_{iaj}^* (13).

Remark 2: Note that τ_j^* and $\bar{\tau}_j^*$ in (18) are piece-wise functions of ρ_{ij} (with at most five cases). Hence, $J_{sH}^*(\rho_{ij})$ in (18) is also a piece-wise function of ρ_{ij}.

Among the remaining control decisions in U_{iaj}^* (13), we have already found the optimal tangential acceleration profile segment $\{u_a^*(t) : t \in \mathscr{P}_{ij}\}$. Integrating this, the corresponding tangential velocity profile segment can be obtained as $v_a^*(t) = \frac{6y_{ij}}{(\rho_{ij}^*)^3}(t - t_o)(t_o + \rho_{ij}^* - t), \ \forall t \in \mathscr{P}_{ij}$. Finally, the optimal angular velocity profile segment $\{w_a^*(t) : t \in \mathscr{P}_{ij}\}$ (required in U_{iaj}^*) can be found using $v_a^*(t)$ in (10) together with the information about the shape of the trajectory segment (i, j).

Remark 3: Note that the OCP (19) (or (17) in general) only requires the total length y_{ij} value of the trajectory segment (i, j). The shape of (i, j) becomes important only when $w_a^*(t)$ has to be determined to facilitate the agent's departure from target i to reach target j (i.e., at the end of an **RHCP3** solving process).

*e) **Solution of RHCP** (14) **for** j^*:* We now have solved RHCP (13) and have obtained the optimal control vector U_{iaj}^* corresponding to the next-visit target j. Next, this process should be repeated for all the neighboring targets $j \in \mathscr{N}_i$ to get the set of control vectors: $\{U_{iaj}^* : j \in \mathscr{N}_i\}$. Finally, the optimal next-visit target j^* can be found from (14) as $j^* = \arg\min_{j \in \mathscr{N}_i} J_H(X_{ia}(t_s), U_{iaj}^*;\ \mathsf{w}(U_{iaj}^*))$.

Upon solving **RHCP3**, the agent a departs from the target i and starts following the trajectory segment (i, j) while executing the obtained optimal agent controls until it arrives at the target j^*. According to the proposed RHC architecture, upon arrival, the agent will solve an instance of **RHCP1**.

*2) Solution of **RHCP1** and **RHCP2**:* Due to space limitations, this topic is omitted here but can be found in [15].

IV. Numerical Results

In this section, we compare the developed RHC solution with respect to the RHC solution proposed in [8]. While both these solutions address the same PMN problem, the former considers the agents as energy-aware and second-order, and the latter assumes the agents as energy-agnostic and first-order. In other words, [8] assumes that each trajectory segment has a predefined transit-time value that an agent has to spend in order to traverse on it, and disregards the energy consumption associated with the agent motion.

The FO-0 curve in Fig. 3 shows the tangential velocity profile over a trajectory segment for such an energy-agnostic first-order agent [8]. Here, the corresponding transit-time ρ_{F0} is predefined. However, note that we can neither characterize the total energy consumption nor control a real-world agent over such velocity profile due to the instantaneous accelerations assumed. Therefore, for this comparison, we approximate the FO-0 curve with the FO-1 curve shown in Fig. 3. In other words, we assume that each agent on each trajectory segment follows a sequence of constant acceleration (of u_{F1}), constant velocity (of v_{F1}) and constant deceleration (of $-u_{F1}$) phases. For convenience, we call this method of controlling agents the "FO-1 Method." The two parameters u_{F1} and v_{F1} are preselected so that each trajectory segment has a fixed transit-time value (see [15] for details).

Let us call the proposed RHC based method of controlling agents with second-order dynamics as the "SO method". In this section, we compare the performance metrics J_T, J_e and J_s defined in (3) obtained for PMN problem configurations (PCs) shown in Fig. 4 under SO and FO-1 methods. These PMN solutions have

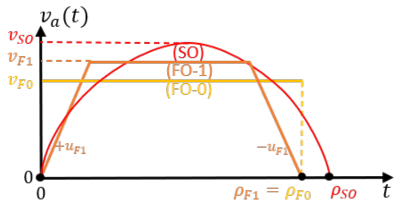

Fig. 3: Tangential agent velocity profiles on a trajectory segment $(i,j) \in \mathscr{E}$ of length y_{ij} under: (i) energy-aware second-order (SO), (ii) energy-agnostic first-order (FO-0) and (iii) energy-agnostic approximate first-order (FO-1) agent control methods (with $t_o = 0$ and $\rho_{F1} = \rho_{F0} = y_{ij}/v_{F0}$).

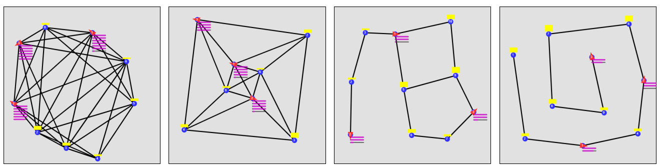

(a) PC1 (b) PC2 (c) PC3 (d) PC4

Fig. 4: Final state of the PMN problem configurations (PCs) after using the highest performing agent control method: SO.

TABLE I: Comparison of performance metrics: J_e, J_s, J_T (3) under SO and FO-1 methods for PMN PCs shown in Fig. 4.

PC	J_T		$J_e \times 10^{-4}$		J_s	
	SO	FO-1	SO	FO-1	SO	FO-1
PC1	1013.9	2090.8	445.9	955.1	62.7	53.2
PC2	705.7	1212.8	306.0	542.6	52.8	55.3
PC3	457.4	776.6	165.7	317.9	103.8	98.5
PC4	432.4	784.4	141.3	314.1	131.0	114.4
Average	**652.4**	1216.2	**264.7**	532.4	87.6	**80.4**

been implemented in a JavaScript based simulator available at `http://www.bu.edu/codes/simulations/shiran27/PersistentMonitoring/`.

In each PC, blue circles represent targets and black lines represent the trajectory segments available for the agents to travel between targets. Yellow vertical bars, purple horizontal bars and red triangles indicate target uncertainty levels, agent energy consumption levels and agent locations (i.e., $R_i(t), J_a(0,t)$ and $s_a(t)$), respectively. The parameters of each PC were chosen as follows: $A_i = 1$, $B_i = 10$, $R_i(0) = 0.5$, $\forall i \in \mathscr{T}$. Targets were placed inside a 600×600 mission space and the time horizon was set to $T = 500$. The initial locations of the agents were chosen such that $s_a(0) = Y_i$ with $i = 1 + (a-1) * \text{round}(M/N)$. The upper bound on the planning horizon (i.e., H) was chosen as $H = \frac{T}{2} = 250$ and the weight factor α in (3) was chosen as $\alpha = 213.3 \times 10^{-6}$.

The obtained comparative results are summarized in Tab. I. According to these results, on average, the energy-aware second-order agents (i.e., the SO method) have outperformed the energy-agnostic (approximate) first-order agents (i.e., FO-1 method) in terms of the energy J_e as well as the total objective J_T by 50.3% and 46.4%, respectively - while only compromising the sensing objective J_s by 9.0%.

V. Conclusion

This paper considers the persistent monitoring problem defined on a network of targets that needs to be monitored by a team of energy-aware dynamic agents. Starting from an existing event-driven receding horizon control (RHC) solution, we exploit optimal control techniques to incorporate agent dynamics and agent energy consumption into the RHC problem setup. The proposed overall RHC solution is computationally efficient, distributed, on-line and gradient-free. Numerical results are provided to highlight the improvements with respect to an RHC solution that uses energy-agnostic first-order agents. Ongoing work aims to determine optimal periodic agent behaviors on networks.

References

[1] M. L. Elwin, R. A. Freeman, and K. M. Lynch, "Distributed Environmental Monitoring with Finite Element Robots," *IEEE Trans. on Robotics*, vol. 36, no. 2, pp. 380–398, 2020.

[2] D. Kingston, R. W. Beard, and R. S. Holt, "Decentralized Perimeter Surveillance Using a Team of UAVs," *IEEE Trans. on Robotics*, vol. 24, no. 6, pp. 1394–1404, 2008.

[3] R. Reshma, T. Ramesh, and P. Sathishkumar, "Security Situational Aware Intelligent Road Traffic Monitoring Using UAVs," in *Proc. of 2nd IEEE Intl. Conf. on VLSI Systems, Architectures, Technology and Applications*, 2016, pp. 1–6.

[4] S. L. Smith, M. Schwager, and D. Rus, "Persistent Monitoring of Changing Environments Using a Robot with Limited Range Sensing," in *Proc. of IEEE Intl. Conf. on Robotics and Automation*, 2011, pp. 5448–5455.

[5] J. Yu, S. Karaman, and D. Rus, "Persistent Monitoring of Events With Stochastic Arrivals at Multiple Stations," *IEEE Trans. on Robotics*, vol. 31, no. 3, pp. 521–535, 2015.

[6] N. Mathew, S. L. Smith, and S. L. Waslander, "Multirobot Rendezvous Planning for Recharging in Persistent Tasks," *IEEE Trans. on Robotics*, vol. 31, no. 1, pp. 128–142, 2015.

[7] S. K. Hari, S. Rathinam, S. Darbha, K. Kalyanam, S. G. Manyam, and D. Casbeer, "The Generalized Persistent Monitoring Problem," in *Proc. of American Control Conf.*, 2019, pp. 2783–2788.

[8] S. Welikala and C. G. Cassandras, "Event-Driven Receding Horizon Control For Distributed Persistent Monitoring in Network Systems," *Automatica*, vol. 127, p. 109519, 2021.

[9] Y.-W. Wang, Y.-W. Wei, X.-K. Liu, N. Zhou, and C. G. Cassandras, "Optimal Persistent Monitoring Using Second-Order Agents with Physical Constraints," *IEEE Trans. on Automatic Control*, vol. 64, no. 8, pp. 3239–3252, 2017.

[10] N. Zhou, C. G. Cassandras, X. Yu, and S. B. Andersson, "Optimal Threshold-Based Distributed Control Policies for Persistent Monitoring on Graphs," in *Proc. of American Control Conf.*, 2019, pp. 2030–2035.

[11] X. Lan and M. Schwager, "Planning Periodic Persistent Monitoring Trajectories for Sensing Robots in Gaussian Random Fields," in *In Proc. of IEEE Intl. Conf. on Robotics and Automation*, 2013, pp. 2415–2420.

[12] N. Rezazadeh and S. S. Kia, "A Sub-Modular Receding Horizon Approach to Persistent Monitoring for A Group of Mobile Agents Over an Urban Area," in *IFAC-PapersOnLine*, vol. 52, no. 20, 2019, pp. 217–222.

[13] J. Kirk, "Traveling Salesman Problem - Genetic Algorithm," 2020. [Online]. Available: https://www.mathworks.com/matlabcentral/fileexchange/13680-traveling-salesman-problem-genetic-algorithm

[14] W. Li and C. G. Cassandras, "A Cooperative Receding Horizon Controller for Multi-Vehicle Uncertain Environments," *IEEE Trans. on Automatic Control*, vol. 51, no. 2, pp. 242–257, 2006.

[15] S. Welikala and C. G. Cassandras, "Event-Driven Receding Horizon Control of Energy-Aware Dynamic Agents for Distributed Persistent Monitoring," *arXiv e-prints*, p. 2102.12963, 2021. [Online]. Available: http://arxiv.org/abs/2102.12963

[16] R. Chen and C. G. Cassandras, "Optimal Assignments in Mobility-on-Demand Systems Using Event-Driven Receding Horizon Control," *IEEE Trans. on Intelligent Transportation Systems*, pp. 1–15, 2020. [Online]. Available: https://doi.org/10.1109/TITS.2020.3030218

[17] J. Yu, M. Schwager, and D. Rus, "Correlated Orienteering Problem and its Application to Persistent Monitoring Tasks," *IEEE Trans. on Robotics*, vol. 32, no. 5, pp. 1106–1118, 2016.

[18] A. E. Bryson, Y. C. Ho, Y. C. Ho, and D. P. Cantwell, *Applied Optimal Control: Optimization, Estimation, and Control*. Hemisphere Publishing Corporation, 1975.